ACS APPLIED MATERIALS & INTERFACES

Research Article

www.acsami.org

Multifunctional Paper Strip Based on Self-Assembled Interfacial Plasmonic Nanoparticle Arrays for Sensitive SERS Detection

Kun Zhang, Jingjing Zhao, Huiying Xu, Yixin Li, Ji Ji,* and Baohong Liu*

Department of Chemistry, State Key Laboratory of Molecular Engineering of Polymers and Institutes of Biomedical Sciences, Fudan University, Shanghai 200433, China

Supporting Information

ABSTRACT: A smart and multifunctional paper-based SERS sensing card is generated through patterning self-assembled interfacial arrays of gold nanoparticles (AuNPs) on the tip of an arrow-shaped paper strip. It is found that the closely packed monolayer of AuNPs is evenly distributed on the paper surface, resulting in a multitude of SERS hot spots over the detection zone. The paper card, with its inherent ability to separate and preconcentrate analytes by the capillary force and polarity difference between sample components, was exploited successfully as an integrated platform, allowing for sub-attomolar (50×10^{-18} M) detection from microliter-volume (10 μL) samples. Furthermore, the simple preparation (lithography-free process), fast detection (<5 min), and low cost (<3 cents) demonstrate that the paper card is a practical and portable sensing interface for wide application in environmental and food analysis.

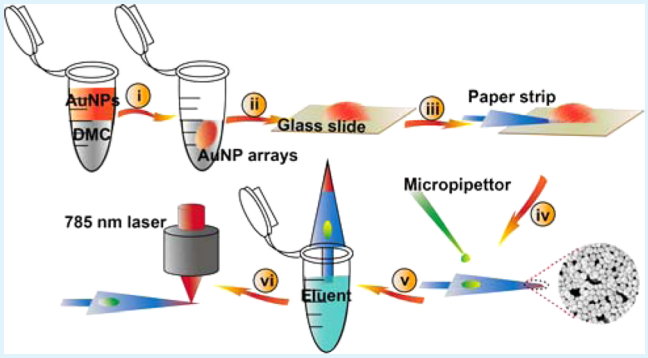

KEYWORDS: *self-assembly, oil/water interface, paper-based sensing device, SERS, multifunction*

INTRODUCTION

Surface-enhanced Raman spectroscopy (SERS) has proven to be an attractive tool for highly sensitive molecular detection of tumor-related biomarkers,[1] pollutants,[2] pesticides,[3] and explosives.[4] For practical applications, it is still a basic focus to fabricate desirable SERS substrates offering multiple advantages of strong Raman enhancement, good reproducibility, and portability. Up until now, extensive efforts have been devoted to preparing various nanostructures for SERS substrates, such as colloidal suspensions of metal nanocrystals using wet chemical synthesis,[5,6] electrochemically roughened metal surfaces,[7] and regularly patterned metal particles on solid surface using vapor deposition,[8,9] lithographic techniques,[10−12] or template-directed self-assembly.[13,14]

Paper, as a versatile and cheap material, has attracted growing interest in recent years for building portable miniature devices that are suitable for developing countries, resource-limited environments, and point-of-care settings.[15−17] Paper-based SERS substrates have also gained considerable attention since they are flexible, inexpensive, efficient for sample collection, and readily disposable. We and others have recently demonstrated the fabrication of low-cost SERS substrates on paper and other flexible materials by inkjet printing,[18] screening printing,[19] soaking,[20] in situ growth,[21,22] and filtration.[23,24] However, limitations in existing paper-based SERS sensors still exist. The inhomogeneous and discrete distribution of nanostructures on paper led to most of these sensors showing only a moderate sensitivity with detection limits at the nanomolar level.[22−25] To improve the signal readout, large sample volumes (milliliter level) are thus needed to accumulate molecular targets in the detection zone, which is impractical for biological and clinical assays.[23,24] Therefore, developing effective and simple access to closely packed nanostructure arrays uniformly distributed on the paper surface is still challenging.

The self-assembled arrays of noble metal nanostructures at a fluid/fluid interface have numerous advantages. They are self-healing, reproducible, and cost-effective.[26] Most importantly, the metal nanoparticles (NPs) within the self-assembled arrays are densely packed and show strong plasmonic coupling, which have been exploited directly into sensitive interfacial SERS sensors.[27−29] The direct in situ SERS measurement on an oil/water interface is limited by the optical configuration of current commercial Raman spectrometers. To address this issue, considerable efforts have been devoted to the development of SERS substrates by transferring the self-assembled NP arrays on various rigid matrixes.[30−32] For example, highly ordered Ag nanowire films assembled at the chloroform/water interface were immobilized on the glass slides for the detection of rhodamine 6G (R6G) molecules at concentrations down to 1×10^{-7} M.[32] We have recently presented a dimethyl carbonate (DMC)/water system that can efficiently organize AuNPs at the oil/water interface without additional "controller" molecules. The formed

Received: May 25, 2015
Accepted: July 17, 2015
Published: July 17, 2015

DOI: 10.1021/acsami.5b04534
ACS Appl. Mater. Interfaces 2015, 7, 16767−16774

Scheme 1. Schematic of the Sensor Development and Sample Detection: (i−iii) Schematic Illustration for Constructing Paper-Based Multifunctional SERS Device by Patterning the Paper Surface with Self-Assembled Interfacial AuNP Arrays; (iv−vi) Simultaneous On-Card Separation, Preconcentration and SERS Detection of Sample Mixture

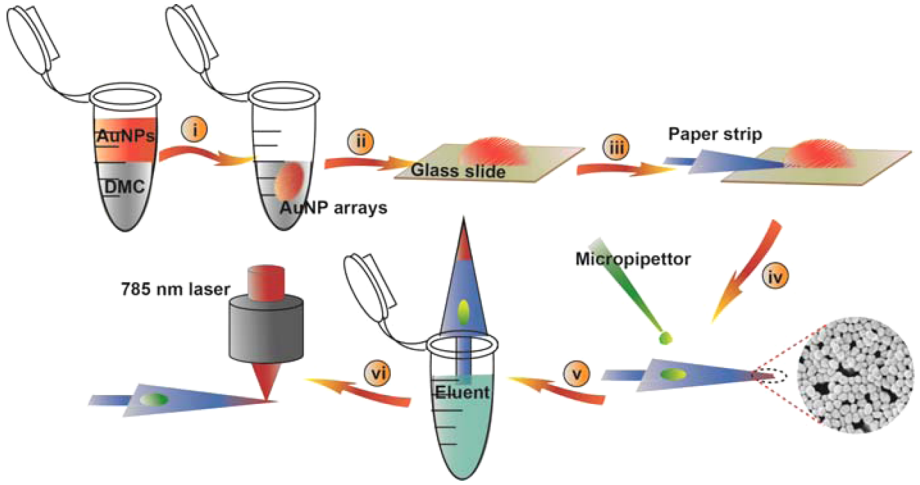

interfacial NP arrays were successfully transferred to a glass substrate and subsequently employed as a simple SERS sensor capable of sensing explosives at sub-femtomolar concentrations.[33] Nevertheless, to the best of our knowledge, there are few reports on the coupling of liquid/liquid self-assembly of NPs with cellulose paper or other flexible materials to construct ultrasensitive SERS-based sensing devices.

Herein, we demonstrate a simple and facile way to construct the SERS-based paper test card by patterning self-assembled AuNP arrays on common chromatographic paper with well-designed geometry. Self-assembly of AuNPs at the DMC/liquid interface was used to conveniently produce a large number of hot spots evenly spread over the paper surface. In realistic situations, the target signals may be interfered with or overwhelmed by coexisting foreign substances with a large Raman cross-section or strong fluorescence emission. Therefore, integrating some important functions such as separation and preconcentration on SERS substrates is highly desirable. In this paper card implementation, the target component can be efficiently separated from sample mixtures based on the polarity differences, and concentrated at the sharp tip of the card by lateral flow when dragged along the paper surface by capillary forces. Considering its high sensitivity, good reproducibility, and low cost, the established SERS-based paper card can be used as a promising multifunctional device for real sample analysis through simultaneous on-card separation, preconcentration, and optical detection.

EXPERIMENTAL SECTION

Reagents and Materials. Chromatography paper (Whatman 1CHR No. 3001-917), chloroauric acid ($HAuCl_4{\cdot}4H_2O$), sodium citrate dihydrate ($Na_3C_6H_5O_7{\cdot}2H_2O$), dimethyl carbonate (DMC), absolute ethanol, acetonitrile, 2,2′- bipyridyl (bpy), rhodamine 6G (R6G), fluorescein, and malachite green (MG) were all purchased from Sinopharm Chemical Reagent Co. Ltd. (Shanghai, China). All of the chemical reagents were of analytical grade and used without any further purification. Ultrapure water (18.2 MΩ·cm) was used through the experiments.

Nanoparticles Preparation. Citrate-stabilized AuNPs were synthesized according to Frens' method.[34] A 50 mL aliquot of $HAuCl_4$ aqueous solution (0.01% by weight) was heated to boiling, and then 0.4 mL of citrate solution (1% by weight) was added under strong stirring. The boiling mixture was continually heated for 15 min to give a brilliant red color indicating the complete reduction of gold(III) ions. The as-prepared AuNPs had a plasmonic band at around 534 nm and an average diameter of 56 nm.

Sensor Fabrication and in Situ SERS Analysis. For construction of the paper-based SERS sensor, we first cut the chromatographic paper into an arrow-shaped geometry (width, 6 mm; length, 20 mm) as the matrix with a sharp tip around 30°. AuNPs were then self-assembled into closely packed arrays by using our previously established DMC/water interfacial system. Typically, AuNPs initially dispersed in water (0.5 mL, ∼35 pM) were induced to migrate toward the oil/liquid (V_{oil}/V_{water}, 2:1) interface through a simple emulsification process. After transferring the produced plasmonic droplet with AuNPs confined at the oil/liquid interface on a cleaned glass slide, the paper substrate was carefully pushed into the droplet followed by removing the extra fluids. The paper-based sensor covered with AuNP arrays was dried sufficiently in air and used in the next-step SERS experiment. A 10 μL aliquot of the sample solution was spotted on the main body of the paper strip followed by drying in air. Afterward, the arrow-like test card was dipped in an appropriate solvent with the rectangular bar to simultaneously separate components with different polarities from the sample mixture and preconcentrate target molecules at the card tip owing to the shape-enhanced capillary-driven flow; i.e., the small tip area resulted in a much faster drying of the solvent at the card tip[35,36] The paper-based sensing device with target molecules effectively concentrated at the plasmon-active top front was then used to conduct the in situ SERS detection by using near-infrared laser (785 nm) excitation as illustrated in Scheme 1.

Characterization. SERS spectra were collected using a Horiba XploRA confocal Raman microspectrometer with 785 nm excitation laser (5 mW laser power). The integration time for each spectrum was set to 10 s with no signal accumulation unless specified otherwise. UV−vis extinction spectra were measured on a PerkinElmer Lambda 750 UV−visible spectrophotometer. Fluorescence spectra were recorded on a Varian Cary Eclipse fluorescence spectrophotometer. Fluorescence images were obtained using a Nikon TE 300 inverted fluorescence microscope. Transmission electron microscopy (TEM) images were obtained using a JEOL JEM-2011 electron microscope at an accelerating voltage of 200 kV. Scanning electron microscopy (SEM) images were obtained using a Hitachi S-4800 filed emission scanning electron microscopy at an accelerating voltage of 1 kV. Atomic force microscope (AFM) images were measured using a Bruker Nanoscope multimode 8 microscope in tapping mode.

RESULTS AND DISCUSSION

Laboratory chromatographic paper (Whatman grade 1) used in this study was composed of microscale (∼15 μm) cellulose fibers interwoven together (Supporting Information Figure S1a). The AFM image demonstrated that the chromatographic paper

DOI: 10.1021/acsami.5b04534
ACS Appl. Mater. Interfaces 2015, 7, 16767−16774

had a hierarchical fibrous morphology with cellulose nanofibers (~20 nm) braided into the large microfibers (Figure S1b). The root-mean-square (RMS) surface roughness of the paper was measured to be 72 nm over a 5 × 5 μm^2 area, well-agreed with the previously reported values,[20] indicating the large surface area of the paper.

Self-assembly of AuNPs at liquid/liquid interfaces was employed to create a uniform plasmon active layer on the paper surface. The citrate-stabilized AuNP suspension had a brilliant red appearance (Figure 1a). After emulsification

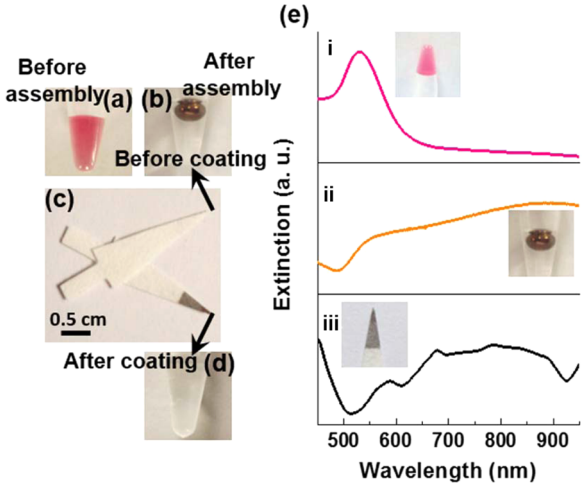

Figure 1. Photographs of AuNPs before (a) and after (b) self-assembly at the DMC/water interface. (c) Photographs of the arrow-like paper card before (top) and after (bottom) loading of AuNP arrays on the top front. (d) Oil phase after coating the paper tip with the self-assembled AuNP arrays. (e) Extinction spectra of individual AuNPs (i), and the interfacial self-assembled AuNP arrays before (ii) and after (iii) loading on the paper tip. Curve ii was obtained by transferring the plasmonic droplet onto a glass slide followed by solvent evaporation. The insets show the corresponding pictures.

(shaking the tube for several seconds) and concentration (pipetting out most of the aqueous phase), nearly all of the particles migrated toward the two-phase interface owing to the minimization of the interfacial energy. This was visually observed by the formation of a water-in-oil droplet with an intense golden metallic appearance in reflected light (Figure 1b) but gray blue when viewed in transmission against a white background (picture not shown). The droplet with AuNPs confined at the interface was easily isolated from the oil as demonstrated previously in our laboratory (Figure 1d). Inserting the chromatographic paper to the interfacial assemblies led to uniform deposition of AuNPs on the paper surface and a color change from white to gray blue (Figure 1c). Figure 1e shows the UV−vis spectra of the interfacial assemblies of AuNPs before and after patterning on the paper surface. The remarkable decrease of the plasmon peak at around 534 nm accompanying the appearance of an intense broad band after 600 nm indicated strong interparticle electronic coupling due to the close arrangement of AuNPs when self-assembling at the DMC/water interface (Figure 1e, curves i and ii. The spectral signature of the NP assemblies-covered paper strip was almost the same as that of the interfacial assemblies (Figure 1e, curve iii, and was totally different from that of bare paper (Figure S2), which implied that AuNPs could be still packed densely after depositing the assemblies on the surface of the paper. This was

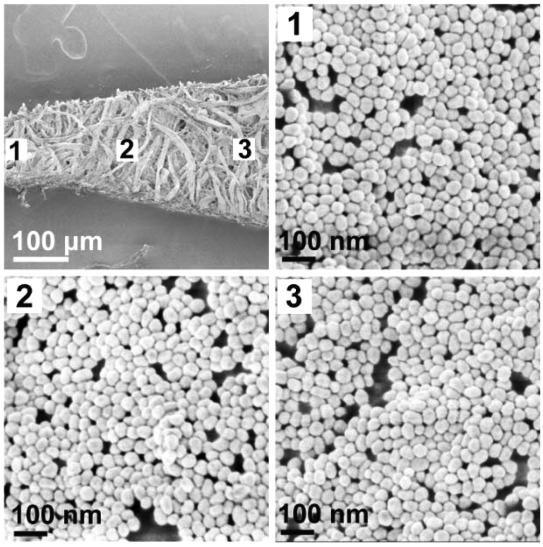

Figure 2. SEM image of the paper substrate coated with interfacial self-assembled AuNP arrays. A zoom at the strip surface shows the close arrangement of nanoparticles at three different spots labeled 1, 2, and 3.

directly revealed by the FE-SEM measurement. As shown in Figure 2, AuNPs covered on the paper surface were closely arranged to form a monolayer of two-dimensional arrays. The surface coverage was estimated to be around 92% by analyzing the SEM image with ImageJ software (U.S. National Institutes of Health). No evidence of the density difference could be clearly observed from different positions on the paper. All of these observations suggested that plenty of electromagnetic hot spots were created and uniformly distributed over the surface of the paper. The entire process for realizing such a high density of particles took less than 3 min, nearly 500 times faster than the conventional immersion method,[20,25] and involved no expensive, electrically powered equipment. It is also of note that autofluorescence of the chromatographic paper was observably suppressed by decoration of the self-assembled AuNP arrays. As can be seen from Figure S3a, the fluorescence spectrum of the paper had two characteristic bands centered at around 487 and 546 nm, respectively, and the fluorescence intensity was quenched by nearly 74% after introduction of the plasmonic layer on the paper. This was further observed by the color variation of the corresponding fluorescence images from green to black (Figure S3b,c). We speculated that the following reasons might contribute to autofluorescence suppression. First, AuNPs could decrease the intrinsic emission of paper via nonradiative energy transfer.[37,38] On the other hand, AuNP assemblies, covered on the paper surface, might inhibit the excitation as well as the collection efficiency of emission photons. All of these were helpful in developing paper into a SERS substrate because the interference coming from the background fluorescence was self-eliminated.

The plasmonic property of metal nanoparticles is known to be highly dependent on the size, shape, and element. Here, ellipsoidal-shaped AuNPs with an average diameter of 56 nm were used as basic units for enabling SERS because of their superior enhancing capability compared with the smaller spherical particles. Figure S4 shows the SERS spectra of 2,2′-bipyridyl collected from the paper surfaces covered respectively with self-assembled arrays of different sizes of AuNPs. Unsurprisingly, the average signal enhancement produced by

DOI: 10.1021/acsami.5b04534
ACS Appl. Mater. Interfaces 2015, 7, 16767−16774

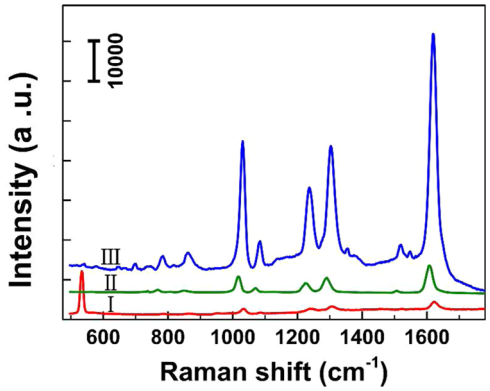

Figure 3. SERS spectra of bpy (1 mM) collected from the surfaces of different substrates. (i) Silicon slide functionalized with AuNPs. (ii) paper-based substrate prepared by immersing paper in the Au colloidal solution for 24 h. (iii) Paper-based substrate fabricated with the interfacial assembled AuNP arrays. The spectra have been vertically offset for clarity.

the 56 nm AuNPs was around 2.5-fold and 8.1-fold larger than that given by 30 and 16 nm AuNPs. It is generally accepted that AgNPs have better SERS performance. In order to elucidate the reason why AuNPs instead of AgNPs were used for the substrate preparation, SERS performance of the paper coated with interfacial assembled AgNP arrays was also investigated. The NP assembly coated paper substrate (around 1.5 × 3 mm^2) was cut off and immersed in the ethanol solution of bpy (1 mM, 100 μL) for 15 min. The substrate was then dried in air and used for SERS analysis with a time interval of 8 days. The SERS intensity of the bpy molecules in this case was about 4-fold less than that from the Au-based surface and showed a continuous decrease to 15% of the initial values after storage for 16 days (Figure S5b). The relatively low signal was presumably because of the lack of coupling of the localized surface plasmon resonance (LSPR) to the laser excitation (785 nm), as these Ag-based structures had LSPRs closer to the shorter wavelength (e.g., 514 nm) in the visible spectral region.[39] The Raman signal attenuation was probably due to the surface oxidation of the patterned Ag arrays under ambient conditions. Conversely, owing to the chemically inert character of AuNPs and the high coverage of them on the paper surface, little change in the intensity of bpy SERS spectrum could be observed even when the substrate was stored in open air for a half-month, indicating excellent stability of the AuNP arrays deposited flexible SERS substrate (Figure S5a).

Figure S6 shows the reproducibility of the paper-based SERS substrate. The SERS spectra of bpy (100 μM) were measured from five randomly selected positions over the NP assembly covered paper surface. The SERS intensity of the band of bpy centered at 1612 cm^{-1} was used for the quantitative evaluation of the signal fluctuation. A relative standard deviation (RSD) of 8.7% for Raman intensities at different positions was obtained, demonstrating the good reproducibility of the plasmonic device described here due to the even coverage of AuNPs on the paper surface. This result was further demonstrated by the highly reproducible signal values measured from different batches of the device (Figure S6b,c) and was comparable to or even better than previously reported literature values for paper-based SERS sensors.[19,25,40]

Having demonstrated the stability and reproducibility of such SERS substrate, we next investigated the signal enhancing

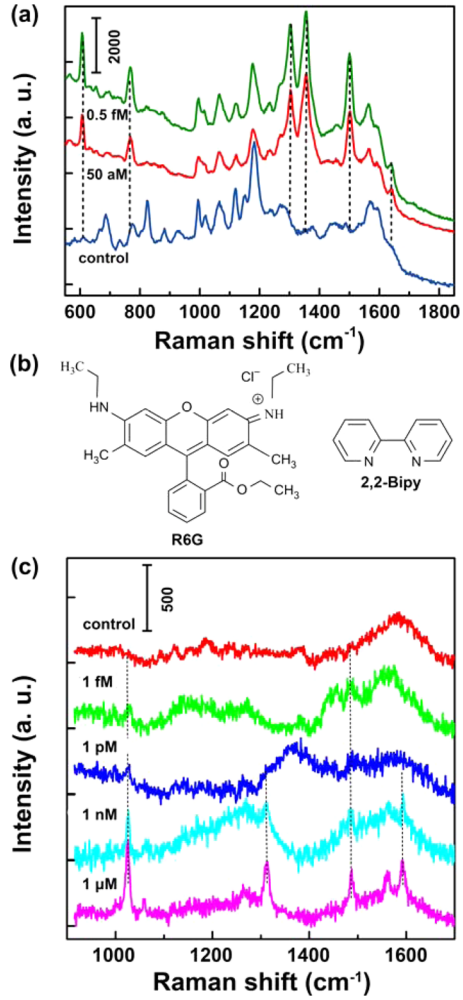

Figure 4. Ultrasensitive SERS analysis of molecules with different Raman sections. (a) Detection of different concentrations of R6G. (b) Molecular structures of R6G and bpy. (c) Detection of different concentrations of bpy.

capability of this paper device by comparing its SERS response with two other types of SERS substrates (silicon slide-based 2D rigid substrate and filter paper-based flexible substrate prepared by the immersion method). The silicon-based substrate was fabricated according to a reference method[41] and was characterized by AFM as shown in Figure S7. The paper substrate made from the self-assembled AuNPs gave highly strong and abundant Raman signals. The band intensity at 1612 cm^{-1} was 8.3-fold larger than that from the immersion-based paper substrate and 36-fold larger than that from the AuNPs-functionalized silicon slide (Figure 3). The superior SERS enhancement was possibly ascribed to the combination of the close proximity induced interparticle coupling and the improved sample collection provided by the flexible cellulose paper.

In order to facilitate the device fabrication and sample detection, the paper card was cut into an arrow-like geometry with a 30° sharp tip down to single fibers. The entire card was 6 mm × 20 mm (maximum width × length). The rationale of this design was that the large area of the main body is convenient for sample loading and migration through the capillary force, whereas the triangular-shaped sharp point is not only beneficial for increasing the local concentration significantly of the analyte of interest but also helpful in eliminating uneven

DOI: 10.1021/acsami.5b04534
ACS Appl. Mater. Interfaces 2015, 7, 16767−16774

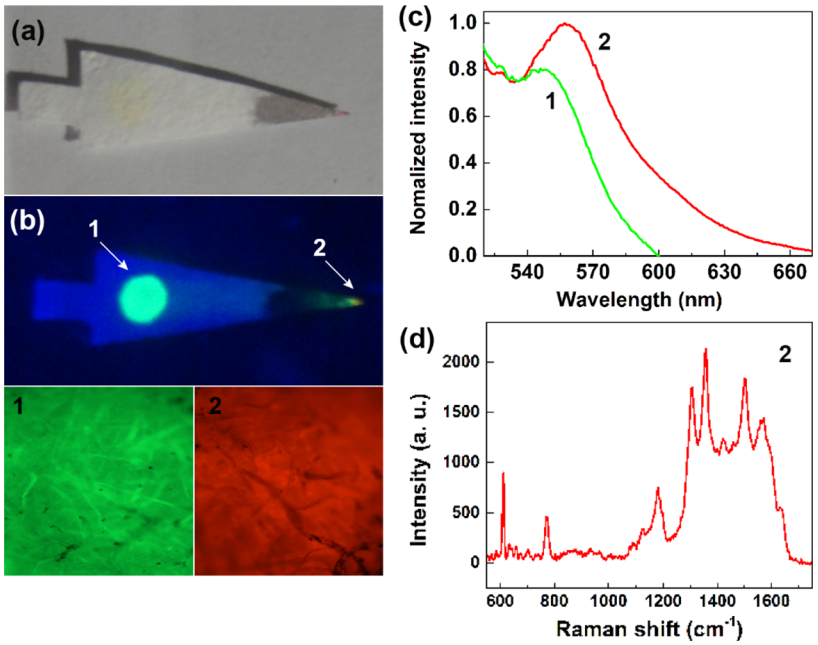

Figure 5. Separation of R6G and fluorescein by the polarity difference and capillary force. Photographs of the paper card after the separation under visible light (a) and UV light (b). Fluorescence images obtained from different positions labeled as 1 and 2 on the paper surface with an excitation filter of 570/40 nm. (c) Fluorescence spectra of fluorescein and R6G measured respectively from the paper surface as shown in b. (d) SERS spectrum of R6G measured from the paper tip after separation.

distribution of detected molecules caused by the coffee ring effect, which is considered as a serious problem for conventional paper-based analytical devices.[42] Thus, the detection ability of the established paper substrate could be further improved by concentrating target molecules to the tiny tip of the plasmonic strip through the lateral flow assay. When the paper strip was wicked up by the capillary action of the cellulose fibers, the analyte molecules were transported to the small detection area (paper tip). R6G was initially used as a model analyte to investigate the effect of preconcentration on the limit of detection (LOD). A 10 μL aliquot of R6G was spotted on the main body of the paper device which was driven to the paper card tip by using acetonitrile as a mobile phase. After drying in air to remove the residual organic solvent, the SERS spectrum was collected on the tip of the paper substrate. As can be seen in Figure 4a, R6G with concentration as low as 50 aM was still clearly detectable, which corresponds to around 300 molecules in the sample solution. To further verify this excellent detection result, bpy with a decreased Raman section was then employed as another analyte. In this case, ethanol was used as the mobile phase considering the lower polarity of bpy. Figure 4b shows the molecular structures of the two compounds. As in the case with R6G, the detection sensitivity was greatly improved with LOD down to 1 fM corresponding to around 6000 molecules, which was lower than the reported values determined from paper-based substrates (Figure 4c).[20,25,40]

The paper-based SERS substrate has also been reported to be used as a simple swab to make the detection of trace analytes feasible.[20,36] Apart from the aforementioned lateral flow concentration-based SERS assay, the developed plasmonic paper card also could be directly used as a SERS swab. Malachite green was first pipetted on the surface of a glass slide, which immediately spread over a circle area with a diameter of around 1 cm. Evaporation of ethanol left residue of MG. A drop of ethanol was placed on the tip of the paper substrate to wet, and then the surface of the glass slide was swabbed to pick up the residue of MG. We collected Raman spectra of the swabbed SERS substrate on six different spots. Figure S8 shows the SERS spectra of MG (1 μM, 10 μL) measured from the two signal acquisition ways. The spectral signatures obtained after the lateral-flow concentration were much stronger than that of the swabbing mode. The band intensity at 416 cm^{-1} clearly revealed that the Raman signal was improved at least 20-fold when determined through the aforementioned microflow mode, which further confirmed the contribution of preconcentration to the increase in the detection sensitivity.

Paper chromatography has been well-established as a quick, facile, and inexpensive way to separate and analyze complex samples.[43,44] Similar to other chromatography techniques, the principle of the separation of components is based on their different affinities for the stationary and mobile phases. To further investigate the separation ability of this platform, we first analyzed a mixture of R6G and fluorescein. A small portion of the mixture (10 μL) was pipetted on the main body of the paper card. After chromatographic separation using a mixed solvent of methanol and water (3:7, v/v) as the mobile phase, the fluorescence spectra and SERS signal were collected to characterize the separation result. It is known that the polarity of R6G is higher compared to that of fluorescein. This polarity difference enables spatially isolating the two dyes on the paper substrate as shown in Figure 5. R6G tends to migrate along the paper surface and concentrate at the tip end owing to the strong interaction with the polar eluent. On the other hand, fluorescein with a decreased polarity has less solubility in the polar mobile phase, resisting any capillary-driven motion to the tip. Interestingly, by simply adjusting the polarity of the mobile phase (methanol/water (7:3, v/v)), we could rapidly separate and concentrate the less polar compound fluorescein from the dye mixture as demonstrated in Figure S9 of Supporting Information.

Based on this principle, a more complex sample composed of R6G spiked in chrysanthemum greens extract was prepared to demonstrate the separation ability of the device for real world

DOI: 10.1021/acsami.5b04534
ACS Appl. Mater. Interfaces 2015, 7, 16767−16774

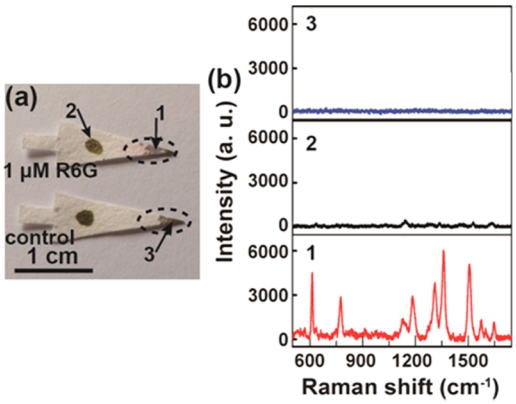

Figure 6. Separation of R6G (1 μM) from the extract of chrysanthemum greens. (a) Photographs of the paper card, either with or without the addition of R6G, after the separation under visible light. (b) SERS spectra obtained from different positions labeled as 1, 2, and 3 on the surfaces of the paper substrate shown in a.

samples. As can be seen in Figure 6, R6G was completely separated from the greens concentrate and dragged to the SERS-active tip by the capillary force, which was clearly observed from the digital photograph and SERS spectra. A control experiment demonstrated that no signals of components of the greens concentrate were detectable at the tip area, suggesting the effectiveness of the device for the separation of more complex samples.

In order to evaluate its application in real samples, the developed SERS-based paper card was used to detect MG in fishpond water, which is a triphenylmethane dye that has been extensively used in aquaculture for prevention and treatment of external fungal and parasitic infections in fish. MG can be readily absorbed by fish tissue and persists in fish muscle and tissues for months, causing carcinogenesis, mutagenesis, chromosomal fractures, teratogenesis, and respiratory toxicity in animals.[45] Conventional methods including HPLC[46] and LC-MS[47] are more instrumentally demanding and expensive to be used for on-site applications. We show the paper card described here as a good alternative to solve those shortcomings. The MG-doped fishpond water was first filtered by passing through a 0.45 μm membrane to remove insoluble particles before the measurement. Figure 7 depicts the SERS spectra of MG with concentrations ranging from 10 fM to 1 μM added in fishpond water. As can be seen from the data, the characteristic peaks at 416 and 433 cm^{-1} assigned to MG could still be clearly identified even at a concentration as low as 10 fM (about 0.004 ppt), which is several orders of magnitude lower than the minimum required performance limit of 2 ppb for the sum of MG and its main metabolite leucomalachite green.[48] Notably, although the SERS intensities were generally positively correlated with the concentrations of MG, the signal fluctuation could be observed from Figure 7. That was probably caused by the complex morphology (3D porous structures) of the paper surface where some AuNP clusters with much enhanced SERS activity might exist and induce the Raman burst at specific locations. Figure S10 shows the UV−vis absorption spectrum of MG aqueous solution; the absorbance maximum was at 619 nm and decreased rapidly to nearly zero as the wavelength increased to around 700 nm that was so far away from the laser wavelength (785 nm) used for SERS excitation. That was to say, the contribution of resonance Raman scattering for the signal amplification of MG molecules could be excluded in our SERS measurements. The high

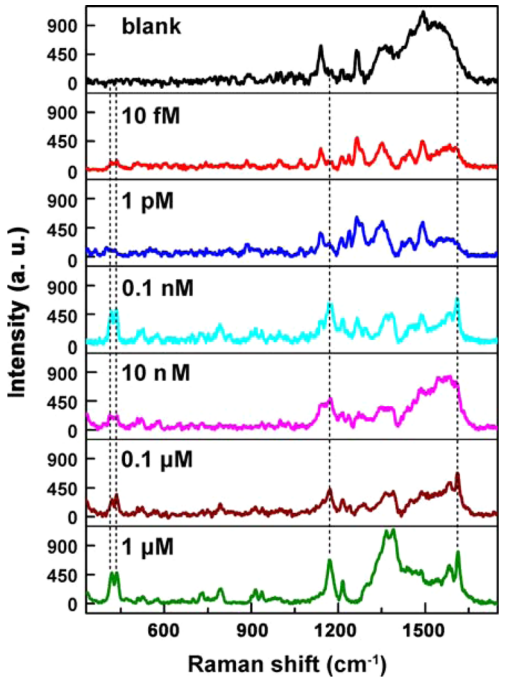

Figure 7. Optical detection of different concentrations of MG in fishpond water using the SERS-based paper test card.

sensitivity mainly came as a result of exciting the surface plasmon resonance of our paper-based SERS substrates.

CONCLUSIONS

In summary, we present a rational designed paper-based sensing device that allows the simultaneous on-card separation, concentration and label-free SERS detection of target molecules from complex samples in a small surface area. The SERS-based paper card has an ultrahigh sensitivity (50 aM of rhodamine can be unambiguously identified) and good separation ability. In addition to the favorable analytical performances, the preparation of the multifunctional SERS sensor is remarkably simple (no sophisticated equipment involved), fast, and cost-effective. Therefore, it has a great potential as a practical sensing platform for applications in environmental and food analysis.

ASSOCIATED CONTENT

Supporting Information

The Supporting Information is available free of charge on the ACS Publications website at DOI: 10.1021/acsami.5b04534.

Additional characterization and spectroscopy data including AFM and fluorescence images and extinction, fluorescence, and SERS spectra (PDF).

AUTHOR INFORMATION

Corresponding Authors

*(B.L.) E-mail: bhliu@fudan.edu.cn.

*(J.J.) E-mail: jiji@fudan.edu.cn.

Notes

The authors declare no competing financial interest.

ACKNOWLEDGMENTS

This work is supported by NSFC (Grants 21375022, 21175028, and 21105014) and the State Key Laboratory of Molecular Engineering of Polymers.

DOI: 10.1021/acsami.5b04534
ACS Appl. Mater. Interfaces 2015, 7, 16767−16774

REFERENCES

(1) Zhang, X.; Zhao, J.; Whitney, A. V.; Elam, J. W.; Van Duyne, R. P. Ultrastable Substrates for Surface-Enhanced Raman Spectroscopy: Al_2O_3 Overlayers Fabricated by Atomic Layer Deposition Yield Improved Anthrax Biomarker Detection. *J. Am. Chem. Soc.* **2006**, *128*, 10304−10309.

(2) Tan, E.-Z.; Yin, P.-G.; You, T.-T.; Wang, H.; Guo, L. Three Dimensional Design of Large-Scale TiO_2 Nanorods Scaffold Decorated by Silver Nanoparticles as SERS Sensor for Ultrasensitive Malachite Green Detection. *ACS Appl. Mater. Interfaces* **2012**, *4*, 3432−3437.

(3) Wang, X. T.; Shi, W. S.; She, G. W.; Mu, L. X.; Lee, S. T. High-Performance Surface-Enhanced Raman Scattering Sensors Based on Ag Nanoparticles-Coated Si Nanowire Arrays for Quantitative Detection of Pesticides. *Appl. Phys. Lett.* **2010**, *96*, 053104.

(4) Yang, L.; Ma, L.; Chen, G.; Liu, J.; Tian, Z. Q. Ultrasensitive SERS Detection of TNT by Imprinting Molecular Recognition Using a New Type of Stable Substrate. *Chem. - Eur. J.* **2010**, *16*, 12683−12693.

(5) He, S.; Liu, K.-K.; Su, S.; Yan, J.; Mao, X.; Wang, D.; He, Y.; Li, L.-J.; Song, S.; Fan, C. Graphene-Based High-Efficiency Surface-Enhanced Raman Scattering-Active Platform for Sensitive and Multiplex DNA Detection. *Anal. Chem.* **2012**, *84*, 4622−4627.

(6) Fales, A. M.; Yuan, H.; Vo-Dinh, T. Silica-Coated Gold Nanostars for Combined Surface-Enhanced Raman Scattering (SERS) Detection and Singlet-Oxygen Generation: A Potential Nanoplatform for Theranostics. *Langmuir* **2011**, *27*, 12186−12190.

(7) Kudelski, A. Raman Studies of Rhodamine 6G and Crystal Violet Sub-Monolayers on Electrochemically Roughened Silver Substrates: Do Dye Molecules Adsorb Preferentially on Highly SERS-Active Sites? *Chem. Phys. Lett.* **2005**, *414*, 271−275.

(8) Chaney, S. B.; Shanmukh, S.; Dluhy, R. A.; Zhao, Y.-P. Aligned Silver Nanorod Arrays Produce High Sensitivity Surface-Enhanced Raman Spectroscopy Substrates. *Appl. Phys. Lett.* **2005**, *87*, 031908.

(9) Semin, D. J.; Rowlen, K. L. Influence of Vapor Deposition Parameters on SERS Active Ag Film Morphology and Optical Properties. *Anal. Chem.* **1994**, *66*, 4324−4331.

(10) Abu Hatab, N. A.; Oran, J. M.; Sepaniak, M. J. Surface-Enhanced Raman Spectroscopy Substrates Created via Electron Beam Lithography and Nanotransfer Printing. *ACS Nano* **2008**, *2*, 377−385.

(11) Green, M.; Liu, F. M. SERS Substrates Fabricated by Island Lithography: The Silver/Pyridine System. *J. Phys. Chem. B* **2003**, *107*, 13015−13021.

(12) Wang, H.; Levin, C. S.; Halas, N. J. Nanosphere Arrays with Controlled Sub-10-nm Gaps as Surface-Enhanced Raman Spectroscopy Substrates. *J. Am. Chem. Soc.* **2005**, *127*, 14992−14993.

(13) Yap, F. L.; Thoniyot, P.; Krishnan, S.; Krishnamoorthy, S. Nanoparticle Cluster Arrays for High-Performance SERS through Directed Self-Assembly on Flat Substrates and on Optical Fibers. *ACS Nano* **2012**, *6*, 2056−2070.

(14) Tessier, P. M.; Velev, O. D.; Kalambur, A. T.; Rabolt, J. F.; Lenhoff, A. M.; Kaler, E. W. Assembly of Gold Nanostructured Films Templated by Colloidal Crystals and Use in Surface-Enhanced Raman Spectroscopy. *J. Am. Chem. Soc.* **2000**, *122*, 9554−9555.

(15) Martinez, A. W.; Phillips, S. T.; Whitesides, G. M.; Carrilho, E. Diagnostics for the Developing World: Microfluidic Paper-Based Analytical Devices. *Anal. Chem.* **2010**, *82*, 3−10.

(16) Martinez, A. W.; Phillips, S. T.; Carrilho, E.; Thomas, S. W., III; Sindi, H.; Whitesides, G. M. Simple Telemedicine for Developing Regions: Camera Phones and Paper-Based Microfluidic Devices for Real-Time, Off-Site Diagnosis. *Anal. Chem.* **2008**, *80*, 3699−3707.

(17) Hu, J.; Wang, S.; Wang, L.; Li, F.; Pingguan-Murphy, B.; Lu, T. J.; Xu, F. Advances in Paper-Based Point-of-Care Diagnostics. *Biosens. Bioelectron.* **2014**, *54*, 585−597.

(18) Yu, W. W.; White, I. M. Inkjet Printed Surface Enhanced Raman Spectroscopy Array on Cellulose Paper. *Anal. Chem.* **2010**, *82*, 9626−9630.

(19) Qu, L.-L.; Li, D.-W.; Xue, J.-Q.; Zhai, W.-L.; Fossey, J. S.; Long, Y.-T. Batch Fabrication of Disposable Screen Printed SERS Arrays. *Lab Chip* **2012**, *12*, 876−881.

(20) Lee, C. H.; Tian, L.; Singamaneni, S. Paper-Based SERS Swab for Rapid Trace Detection on Real-World Surfaces. *ACS Appl. Mater. Interfaces* **2010**, *2*, 3429−3435.

(21) Cheng, M.-L.; Tsai, B.-C.; Yang, J. Silver Nanoparticle-Treated Filter Paper as a Highly Sensitive Surface-Enhanced Raman Scattering (SERS) Substrate for Detection of Tyrosine in Aqueous Solution. *Anal. Chim. Acta* **2011**, *708*, 89−96.

(22) Meng, Y.; Lai, Y.; Jiang, X.; Zhao, Q.; Zhan, J. Silver Nanoparticles Decorated Filter Paper via Self-Sacrificing Reduction for Membrane Extraction Surface-Enhanced Raman Spectroscopy Detection. *Analyst* **2013**, *138*, 2090−2095.

(23) Yu, W. W.; White, I. M. A Simple Filter-Based Approach to Surface Enhanced Raman Spectroscopy for Trace Chemical Detection. *Analyst* **2012**, *137*, 1168−1173.

(24) Zhang, K.; Ji, J.; Fang, X.; Yan, L.; Liu, B. Carbon Nanotube/Gold Nanoparticle Composite-Coated Membrane as a Facile Plasmon-Enhanced Interface for Sensitive SERS Sensing. *Analyst* **2015**, *140*, 134−139.

(25) Lee, C. H.; Hankus, M. E.; Tian, L.; Pellegrino, P. M.; Singamaneni, S. Highly Sensitive Surface Enhanced Raman Scattering Substrates Based on Filter Paper Loaded with Plasmonic Nanostructures. *Anal. Chem.* **2011**, *83*, 8953−8958.

(26) Edel, J. B.; Kornyshev, A. A.; Urbakh, M. Self-Assembly of Nanoparticle Arrays for Use as Mirrors, Sensors, and Antennas. *ACS Nano* **2013**, *7*, 9526−9532.

(27) Booth, S. G.; Cowcher, D. P.; Goodacre, R.; Dryfe, R. A. W. Electrochemical Modulation of SERS at the Liquid/Liquid Interface. *Chem. Commun.* **2014**, *50*, 4482−4484.

(28) Kim, K.; Han, H. S.; Choi, I.; Lee, C.; Hong, S.; Suh, S.-H.; Lee, L. P.; Kang, T. Interfacial Liquid-State Surface-Enhanced Raman Spectroscopy. *Nat. Commun.* **2013**, *4*, 2182.

(29) Cecchini, M. P.; Turek, V. A.; Paget, J.; Kornyshev, A. A.; Edel, J. B. Self-Assembled Nanoparticle Arrays for Multiphase Trace Analyte Detection. *Nat. Mater.* **2013**, *12*, 165−171.

(30) Fontana, J.; Livenere, J.; Bezares, F. J.; Caldwell, J. D.; Rendell, R.; Ratna, B. R. Large Surface-Enhanced Raman Scattering from Self-Assembled Gold Nanosphere Monolayers. *Appl. Phys. Lett.* **2013**, *102*, 201606.

(31) Tanoue, Y.; Sugawa, K.; Yamamuro, T.; Akiyama, T. Densely Arranged Two-Dimensional Silver Nanoparticle Assemblies with Optical Uniformity over Vast Areas as Excellent Surface-Enhanced Raman Scattering Substrates. *Phys. Chem. Chem. Phys.* **2013**, *15*, 15802−15805.

(32) Shi, H.-Y.; Hu, B.; Yu, X.-C.; Zhao, R.-L.; Ren, X.-F.; Liu, S.-L.; Liu, J.-W.; Feng, M.; Xu, A.-W.; Yu, S.-H. Ordering of Disordered Nanowires: Spontaneous Formation of Highly Aligned, Ultralong Ag Nanowire Films at Oil−Water−Air Interface. *Adv. Funct. Mater.* **2010**, *20*, 958−964.

(33) Zhang, K.; Ji, J.; Li, Y.; Liu, B. Interfacial Self-Assembled Functional Nanoparticle Array: A Facile Surface-Enhanced Raman Scattering Sensor for Specific Detection of Trace Analytes. *Anal. Chem.* **2014**, *86*, 6660−6665.

(34) Frens, G. Controlled Nucleation for the Regulation of the Particle Size in Monodisperse Gold Suspensions. *Nature, Phys. Sci.* **1973**, *241*, 20−22.

(35) Abbas, A.; Brimer, A.; Slocik, J. M.; Tian, L.; Naik, R. R.; Singamaneni, S. Multifunctional Analytical Platform on a Paper Strip: Separation, Preconcentration, and Subattomolar Detection. *Anal. Chem.* **2013**, *85*, 3977−3983.

(36) Yu, W. W.; White, I. M. Inkjet-Printed Paper-Based SERS Dipsticks and Swabs for Trace Chemical Detection. *Analyst* **2013**, *138*, 1020−1025.

(37) Dulkeith, E.; Morteani, A. C.; Niedereichholz, T.; Klar, T. A.; Feldmann, J.; Levi, S. A.; van Veggel, F. C. J. M.; Reinhoudt, D. N.; Möller, M.; Gittins, D. I. Fluorescence Quenching of Dye Molecules near Gold Nanoparticles: Radiative and Nonradiative Effects. *Phys. Rev. Lett.* **2002**, *89*, 203002.

DOI: 10.1021/acsami.5b04534
ACS Appl. Mater. Interfaces 2015, 7, 16767−16774

(38) Singamaneni, S.; Jiang, C.; Merrick, E.; Kommireddy, D.; Tsukruk, V. V. Robust Fluorescent Response of Micropatterned Multilayered Films. *J. Macromol. Sci., Part B: Phys.* **2007**, *46*, 7−19.
(39) Sherry, L. J.; Chang, S.-H.; Schatz, G. C.; Van Duyne, R. P.; Wiley, B. J.; Xia, Y. Localized Surface Plasmon Resonance Spectroscopy of Single Silver Nanocubes. *Nano Lett.* **2005**, *5*, 2034−2038.
(40) Qu, L.-L.; Song, Q.-X.; Li, Y.-T.; Peng, M.-P.; Li, D.-W.; Chen, L.-X.; Fossey, J. S.; Long, Y.-T. Fabrication of Bimetallic Microfluidic Surface-Enhanced Raman Scattering Sensors on Paper by Screen Printing. *Anal. Chim. Acta* **2013**, *792*, 86−92.
(41) Lu, L.; Sun, G.; Zhang, H.; Wang, H.; Xi, S.; Hu, J.; Tian, Z.; Chen, R. Fabrication of Core-Shell Au-Pt Nanoparticle Film and Its Potential Application as Catalysis and SERS Substrate. *J. Mater. Chem.* **2004**, *14*, 1005−1009.
(42) Määttänen, A.; Fors, D.; Wang, S.; Valtakari, D.; Ihalainen, P.; Peltonen, J. Paper-Based Planar Reaction Arrays for Printed Diagnostics. *Sens. Actuators, B* **2011**, *160*, 1404−1412.
(43) Li, H.; Qiu, T.; Cao, Y.; Yang, J.; Huang, Z. Pre-Staining Paper Chromatography Method for Quantification of γ-Aminobutyric Acid. *J. Chromatogr. A* **2009**, *1216*, 5057−5060.
(44) Pandey, U.; Dhami, P. S.; Jagesia, P.; Venkatesh, M.; Pillai, M. R. A. Extraction Paper Chromatography Technique for the Radionuclidic Purity Evaluation of ^{90}Y for Clinical Use. *Anal. Chem.* **2008**, *80*, 801−807.
(45) Srivastava, S.; Sinha, R.; Roy, D. Toxicological Effects of Malachite Green. *Aquat. Toxicol.* **2004**, *66*, 319−329.
(46) Mitrowska, K.; Posyniak, A.; Zmudzki, J. Determination of Malachite Green and Leucomalachite Green in Carp Muscle by Liquid Chromatography with Visible and Fluorescence Detection. *J. Chromatogr. A* **2005**, *1089*, 187−192.
(47) Scherpenisse, P.; Bergwerff, A. A. Determination of Residues of Malachite Green in Finfish by Liquid Chromatography Tandem Mass Spectrometry. *Anal. Chim. Acta* **2005**, *529*, 173−177.
(48) Guo, Z.; Gai, P.; Hao, T.; Duan, J.; Wang, S. Determination of Malachite Green Residues in Fish Using a Highly Sensitive Electrochemiluminescence Method Combined with Molecularly Imprinted Solid Phase Extraction. *J. Agric. Food Chem.* **2011**, *59*, 5257−5262.

DOI: 10.1021/acsami.5b04534
ACS Appl. Mater. Interfaces 2015, 7, 16767−16774